Stress Fibers in Cells *in Situ*: Immunofluorescence Visualization with Antiactin, Antimyosin, and Anti-alpha-actinin

H. RANDOLPH BYERS and KEIGI FUJIWARA
Department of Anatomy, Harvard Medical School, Boston, Massachusetts 02115

ABSTRACT Stress fiber-like patterns are visualized by indirect immunofluorescence in scleroblasts (fibroblasts) *in situ* on the scale of the common goldfish, *Carassius auratus*, using an affinity-purified antiactin, antimyosin, and anti-alpha-actinin. These fibers demonstrate the classical convergent and parallel patterns exhibited by stress fibers in tissue culture cells. Because the dimensions, the composition, and the pattern of distribution of these cytoplasmic fibers correspond well with those of stress fibers in cultured cells, we will call these fibers stress fibers also. The staining patterns with anti-alpha-actinin and antimyosin along the stress fibers often reveal a periodicity of 1–2 μm, identical to that found in cells in vitro. The majority of scleroblasts do not exhibit stress fiber staining and they are specifically located in the central regions of the scale. Stress fibers are present in scleroblasts residing on or near the edges or radical ridges of the scale. They are consistently orientated perpendicular to these structures; however, unlike microtubules, stress fibers show no co-alignment with collagen fibers of the scale. The finding that stress fibers are lcoated in regions of the scale more subject to shearing forces may indicate their role in increased cellular adhesion to the substratum.

Stress fibers have been observed in cultured living cells at the light microscope level (3, 14). Ultrastructurally they are composed of bundles of actin filaments (19). Fluorescent antibody staining have revealed that many contractile proteins exhibit a specific localization pattern along the stress fiber. The fluorescent staining pattern of antiactin (17, 27) is continuous throughout the length of stress fibers; however, the staining with antimyosin (11), antitropomyosin (25), and anti-alpha-actinin (26) is often periodic. Microinjection studies of fluorescently labeled actin (22) and alpha-actinin (9) into living cultured cells also reveal similar fluorescent patterns in the stress fiber.

Studies on stress fibers in cells in vitro have suggested that these fibers may play a role in cell spreading and attachment to the substratum (1, 3, 27, 37), directed migration or locomotion (33), in vitro wound healing (16), and the behavior of transformed cells (15). To help evaluate the biological significance of the voluminous research on stress fibers in cultured cells, it is important to ask whether stress fibers are epiphenomena or artifacts of cells in tissue culture. To determine whether stress fibers actually exist in cells *in situ*, we used a tissue that has recently been amenable to immunofluorescent visualization of microtubules *in situ* (6). In this tissue, fibroblast cells, called scleroblasts, reside as a thin monolayer on the surface of the fibrillary plate of the fish scale (20, 29). On the underside of the scale the scleroblasts are not covered by epidermal cells and can, thus, be directly visualized.

We demonstate by immunofluorescence techniques that stress fibers are present in cells of a highly differentiated tissue *in situ*. Although the majority of scleroblasts do not exhibit stress fibers, cells adjacent to the edge of the scale do contain stress fibers. These stress fibers are oriented nearly perpendicular to the edge of the scale. Since the borders of fish scales are likely to be subject to greater shearing forces than central regions, the presence of stress fibers in cells in this region may enhance cellular adhesion to the substratum.

MATERIALS AND METHODS

Preparation of Antiactin Antiserum

ANTIGEN: The marine fish, *Stenotomus versicolor*, or common scup, were sacrificed by spinal section after ice-water cold shock. Acetone powder was made from ~100 g of the fresh muscle (34). Actin extracted from the acetone powder was first enriched by the cyclic polymerization and depolymerization procedure (34) and then purified by Sephadex G-150 column chromatography (17). Fractions containing actin were analyzed by 7.5% PAGE in SDS. The gels were stained with Coomassie Brilliant Blue and scanned at 550 nm. Purified actin was lyophilized and stored dry at −20°C.

THE JOURNAL OF CELL BIOLOGY · VOLUME 93 JUNE 1982 804-811

IMMUNIZATION: Lyophilized actin was dissolved in buffer A (34) to a concentration of 1 mg/ml and polymerized by increasing the salt concentration to 100 mM KCl and 2 mM $MgCl_2$. The F-actin was fixed by 0.1% glutaraldehyde (Taab Labs, Berkshire, England) for 1 h at room temperature and dialyzed for 24 h against several changes of phosphate-buffered saline (PBS) containing 0.85% NaCl, 10 mM Na-phosphate at pH 7.3. Two white New Zealand female rabbits were each injected subcutaneously with 350 μg of actin, emulsified with complete Freund's adjuvant (Gibco 17-5721; Grand Island Biological Co., Grand Island, NY), along two shaved panels on the rabbit's back. An additional rabbit was injected with 350 μg of native polymerized actin emulsified with Freund's adjuvant. After 4 wk the rabbits were boosted with either 350 μg of glutaraldehyde-fixed F-actin or 400 μg of native F-actin emulsified with incomplete Freund's adjuvant (Gibco 660-5720). The rabbits were bled from ear veins to obtain 50 ml of blood on days 5, 7, 9, and 11 after the boost. Immunoglobulin G (IgG) was fractionated by ammonium sulfate at 40% saturation, redissolved in half the original serum volume of PBS, dialyzed against PBS for at least 1.5 d with three changes of PBS, and stored either frozen at −20°C or at 4°C in PBS with 0.02% NaN_3.

Purification and Characterization of Antiactin

Initial Screening

Presence of antiactin in antisera or IgG fractions of antisera was tested by double immunodiffusion against extracts of fish skeletal muscle acetone powder and human platelet and column-purified fish skeletal muscle actin. Initial testing for the presence of nonprecipitating antibodies was the staining of stress fibers and the I-band in myotubes of embryonic chick primary cultures by indirect immunofluorescence.

Affinity Chromatography

The purification of antiactin antibody by affinity column chromatography (17) was carried out using slight modification. Briefly, 10 mg of purified actin was dialyzed against 0.2 mM $CaCl_2$, 0.1 M KCl, 10 mM Na-phosphate at pH 9.5, and coupled to 4 ml of wet Sepharose 4B beads (Pharmacia Fine Chemicals, Piscataway, NJ) that were activated by cyanogen bromide (7). Ammonium sulfate-fractionated immune IgG was chromatographed on DEAE cellulose (Whatman DE52) equilibrated with 10 mM Na-phosphate buffer, pH 7.5 (11). The IgG eluting at 40 mM NaCl (100 mg IgG/35 ml) was dialyzed against PBS and gently stirred with the actin-bound Sepharose beads for no more than 2 h at 4°C. The beads were poured into a small column and washed with PBS to remove the unbound IgG until no absorbance was detected at 280 nm. This fraction is defined as absorbed IgG. The bound IgG was eluted with 0.2 M glycine at pH 2.8 and stored as described previously (11).

Characterization of Affinity-purified Antiactin

NITROCELLULOSE DISK-TECHNIQUE: Several disks (6-mm diameter) were cut from a nitrocellulose sheet (HA, 0.45 μm; Millipore Corp., Bedford, MA) and attached to a petri dish with double-stick tape. 5 μl of solution (1 mg/ml) containing purified fish skeletal actin, human platelet actin, or chicken gizzard tropomyosin was applied to the center of a disk and allowed to dry. The disks were then flooded with PBS containing 3% bovine serum albumin (BSA) and 1% normal goat serum (NGS) and incubated for 15 min. They were rinsed twice in PBS for 2 min each and incubated for 30 min with 20 μl of varying concentrations of either affinity-purified antiactin or absorbed IgG. Antibodies bound to the disk were visualized by the peroxidase-antiperoxidase (PAP) procedure described below.

ELECTROPHORESIS BLOTTING TECHNIQUE: The specificity of the antiactin was determined by modifications of the electrophoretic blotting technique (35). Crude fish skeletal muscle extracts, twice-cycled pig brain microtubule proteins, and known protein standards including purified actin were loaded onto an SDS-containing slab gel and electrophoresed using 5% stacking and 7.5% separating gels (24). The gels were removed and rinsed quickly in a modified electrode buffer containing 20% methanol and no SDS. An aluminium-foil-covered glass plate was placed flat in a shallow plastic tray and was connected to the positive electrode of the power supply. A Whatman no. 1 filter paper was placed on the plate and saturated with the modified electrode buffer. All subsequent interfaces were also generously wetted with this buffer. We laid a nitrocellulose sheet over the filter paper, taking care to avoid bubbles. The polyacrylamide gel was carefully placed over the nitrocellulose, which was followed by another Whatman filter paper. Another aluminium-foil-covered glass plate (negative electrode) was placed over the multiple layers, two 1-mm Teflon strips were interposed between the plates on either side of the gel, and the top plate was held down with an ~200-g mass. The gel bands were then electrophoresed onto the nitrocellulose by running at 1.5–2.0 V (16–30 mA) for 1 h. The nitrocellulose was cut into strips corresponding to the gel lanes, and, to confirm the successful transfer of proteins, a few strips were stained with 0.1% amido black in 45% methanol, 10% acetic acid for 5–15 min, and destained with 90% methanol and 2% acetic acid for 20 min. The nitrocellulose strips that were not stained with amido black were incubated for 1 h with 3% BSA and 1% NGS in PBS at 25°C. The strips were rinsed twice in PBS and incubated for 30 min in 50 μl of affinity-purified antibody (100 μg/ml) or absorbed IgG (500 μg/ml) in 3% BSA in PBS. The PAP procedure described below was used to detect bound antibodies.

PAP PROCEDURE: The nitrocellulose disks and strips were washed five times for 2 min each with PBS and incubated for 30 min with a 1:20 dilution of goat anti-rabbit serum (lot 5091; Sternberger-Meyer Immunocytochemicals, Inc., Jarrettsville, MD) in 1% NGS. After five washes in PBS as described above, a 1:500 dilution of rabbit PAP complex (Sternberger-Meyer lot 5004) in 1% NGS was applied for 30 min. The final five 2-min rinses were carried out using a 50 mM Tris-Cl buffer, pH 7.6, instead of PBS. The strips were soaked in the reaction solution containing 0.05% 3,3′-diaminobenzidine (grade II; Sigma Chemical Co., St. Louis, Mo) and 0.01% H_2O_2 for 5–10 min or until the brown reaction product was clearly visible. The reaction is stopped by adding an excess amount of distilled H_2O.

Preparation of Antimyosin and Anti-alpha-actinin

A detailed description of the preparation and characterization of antibodies to myosin (11) and alpha-actinin (12) can be found in earlier publications.

Preparation and Staining of Tissue Culture Cells

Primary culture cells from 11-d-old embryonic chick and 3T3 cells were grown on glass cover slips with Eagle's basal medium with 10% fetal calf serum for 3–5 d. The cells were fixed for 15 min in 3.7% formaldehyde with 1 mM EGTA, 1 mM $MgCl_2$ in PBS. They were rinsed three times in PBS with 0.2% Triton X-100 for 2 min. After another three rinses in PBS, the cells were incubated with 30 μl of affinity-purified antiactin antibody (50 μg/ml) for 45 min. After three rinses in PBS, the cover slips were incubated for 45 min with 30 μl of a 1:250 dilution of fluorescein-conjugated goat anti-rabbit IgG (Fl-GAR) (Miles Yeda, Inc., Rehovot, Israel). After the final rinses in PBS, the cover slips were mounted in 25% glycerol, 10 mM Tris-HCl, pH 9.0, 0.02% NaN_3.

Preparation and Staining of Cells in Situ

Scales from the common goldfish, *Carassius auratus*, were removed with fine forceps and immediately fixed with 3.7% formaldehyde, 1 mM EGTA, 1 mM $MgCl_2$ in PBS for 30 min. The scales were incubated with 3% BSA in PBS for 15 min to reduce nonspecific background staining, followed by three rinses in PBS for a total of 5 min. The membranes were rendered permeable by treatment with 0.2% Triton X-100 for 4 min and then rinsed in PBS three times as before. Indirect immunofluorescence procedures (6) were carried out on different scales with the following antibodies: affinity-purified antiactin (50 μg/ml), a 1:20 dilution of serum containing antimyosin, and a 1:20 dilution of anti-alpha-actinin serum.

Controls for Indirect Immunofluorescence

Fixed and permeabilized fish scales and cultured cells were incubated (*a*) with the absorbed IgG and then Fl-GAR, (*b*) with preimmune serum and Fl-GAR, (*c*) with Fl-GAR alone, or (*d*) with antiactin and then unlabeled GAR followed by Fl-GAR. In addition, the various cell types in the scale were examined for any autofluorescence after formaldehyde fixation. Controls for the antimyosin and anti-alpha-actinin staining of the fish scale were carried out as for the controls for the antiactin staining described above.

Microscopy and Photomicroscopy

Observation of fluorescent staining was carried out by use of a Leitz microscope (Orthoplan) equipped with a Xenon lamp (XBO-150, Xenon Corp., Watertown, MA), a Ploemopak 2 illuminator containing a Leitz L-2 filter block and a Zeiss 63× planapo phase-objective lens (N.A. 1.4, oil). For phase-contrast microscopy, a Leitz phase contrast condensor was fitted with a phase ring matching the Zeiss lens. Photomicrographs are taken with a Leitz automatic camera (Orthomat-W) using Kodak 35-mm Tri-X film. The film was pushed to ASA 1000 by development in Acufine (Acufine, Inc., Chicago, IL). To determine the shape of scleroblasts on the scale, we used Zeiss UEM stand equipped with Nomarski differential interference contrast system and a 63X planapo phase-

contrast lens (N.A. 1.4, oil). The photographs were taken using Kodak Pan X and Zeiss automatic exposure system (MC63).

RESULTS

Column-purified Actin

When twice-cycled fish skeletal muscle actin was chromatographed on a Sephadex G-150 column, two distinct peaks were obtained. Both components were determined to be actin by SDS PAGE. The faster running component (20% of the total protein) was thus assumed to consist of actin oligomers. The peak fractions of the second component (80% of the total protein) were used to inject the rabbits and to construct the affinity column. An SDS gel of the second peak fractions is shown in Fig. 1 *a*, and the purity of the fraction was >99% as determined by scanning stained gels.

Characterization and Purification of the Antiactin Antisera

Of three rabbits injected, only one rabbit immunized with glutaraldehyde-fixed F-actin produced antiserum that demonstrated stress-fiber staining after the initial or secondary boost. However, this antiserum did not form precipitin lines against purified actin, crude extracts of the original fish skeletal muscle, or extracts from human platelets as determined by Ouchterlony analysis or immunoelectrophoresis. Affinity-purified antiactin antibodies also failed to form precipitin lines.

The presence of nonprecipitating antiactin was detected by the nitrocellulose disk technique (Fig. 1 *b*), and the specificity of the antiactin was established by the electrophoretic blotting technique (Fig. 2 *c*). In Fig. 1 *b*, purified fish skeletal muscle actin was adsorbed to disks *1* through *5*, while human platelet actin and chicken gizzard tropomyosin were loaded onto disks *6* and *7*, respectively. Disks *1* and *2* were reacted with absorbed IgG and show little or no peroxidase reaction product. Intense staining was present in disks *3* (250 μg/ml antiactin), *4* (100 μg/ml antiactin), and *5* (10 μg/ml antiactin). The antibodies against fish skeletal muscle actin reacted with human platelet actin (disk *6*) and did not bind to tropomyosin (disk *7*).

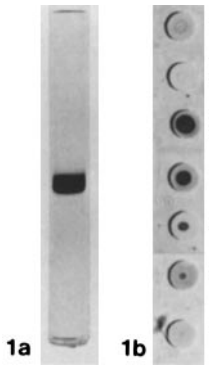

FIGURE 1 Antigen preparation and characterization of antiactin. (*a*) Coomassie Brilliant Blue-stained polyacrylamide gel of column purified fish skeletal muscle actin. 100 μg of protein is loaded. (*b*) Characterization of nonprecipitating antiactin by nicrocellulose disk technique. Purified antigens (5 μg) are adsorbed onto nitrocellular disks, and the PAP staining procedure is carried out after the disks are incubated with 0.1 ml of either affinity-purified antiactin or absorbed IgG. The absorbed antigen and the immunological reagent for each disk are: disk *1*, fish skeletal muscle actin and absorbed IgG (0.37 mg/ml); disk *2*, fish skeletal muscle actin and absorbed IgG (0.037 mg/ml); disk *3*, fish skeletal muscle actin and antiactin (0.25 mg/ml); disk *4*, fish skeletal muscle actin and antiactin (0.10 mg/ml); disk *5*, fish skeletal muscle actin and antiactin (0.01 mg/ml); disk *6*, human platelet actin and antiactin (0.25 mg/ml); disk *7*, chicken gizzard tropomyosin and antiactin (0.25 mg/ml). Disks *3–6* show reaction products, while disks *1*, *2*, and *7* do not. The antiactin made against fish skeletal muscle actin cross-reacts with human platelet actin (disk *6*). There are no detectable antibodies to tropomyosin, a likely contaminant in the original actin preparation (disk *7*). The size of the stained area is not quantitative and relates only to the spread of the antigen solution during the adsorption process.

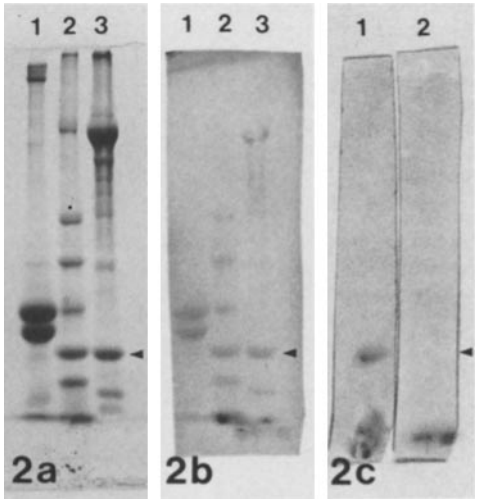

FIGURE 2 Characterization of antiactin by electrophoretic-blotting technique. (*a*) Coomassie Brilliant Blue-stained polyacrylamide slab gel of twice-cycled pig brain microtubule proteins (lane *1*), protein standards (lane *2*) containing myosin heavy chain (200,000), phosphatase A (95,000), bovine serum albumin (68,000), catalase (60,000), actin (42,000), and aldolase (40,000), and fish skeletal muscle extract (lane *3*). (*b*) Amido-black-stained nitrocellulose strip containing electrophoretically transferred proteins from a gel similar to *a*. (*c*) Nitrocellulose strips similar to lane *3* in *b* containing transferred fish skeletal muscle proteins are stained by the PAP procedure using antiactin (strip *1*) and absorbed IgG (strip *2*). The actin band in strip *1* is stained. The reaction product at the dye front is nonspecific. The position of actin band is indicated by arrowheads.

Fig. 2 *a* is a polyacrylamide slab gel stained with Coomassie Blue and shows electrophoretic patterns of twice-cycled porcine brain microtubule proteins (lane *1*), protein standard (lane *2*), and crude fish skeletal muscle extract (lane *3*). The arrowhead indicates the position of actin. A similar, but unstained, slab gel was used to transfer protein bands to a nitrocellulose strip. When such a strip was stained with amido black (Fig. 2 *b*), most of the major bands could be identified, including actin (arrowhead). However, because transfer efficiency was low and the amido black is less sensitive than the Coomassie Blue, minor bands are not detectable (compare Fig. 2 *a* and *b*). High molecular weight components such as the microtubule-associated proteins (Fig. 2 *b*, lane *1*) and myosin (Fig. 2 *b*, lanes *2* and *3*) were particularly poorly transferred.

When an unstained nitrocellulose strip similar to lane *3* of Fig. 2 *b* was reacted with affinity-purified antiactin and processed through the PAP procedure, only the actin band (arrowhead) showed an intense reaction product (Fig. 2 *c*, strip *1*). No staining was observed when absorbed IgG was used instead of antiactin (Fig. 2c, strip *2*). The area around the dye front always showed some nonspecific reaction product.

When embryonic chick tissue culture cells or 3T3 cells were stained with affinity-purified antiactin and Fl-GAR, cells exhibited fluorescence patterns similar to those of antiactin staining reported by other investigators (17, 27). Fig. 3 *a* shows fluorescently labeled parallel and convergent stress fibers, the ruffling cell perimeter, and diffuse perinuclear cytoplasmic staining of cultured embryonic chick cells. Lamellipodia, when present, also stained brightly. These staining patterns were immunologically specific, because the four control experiments

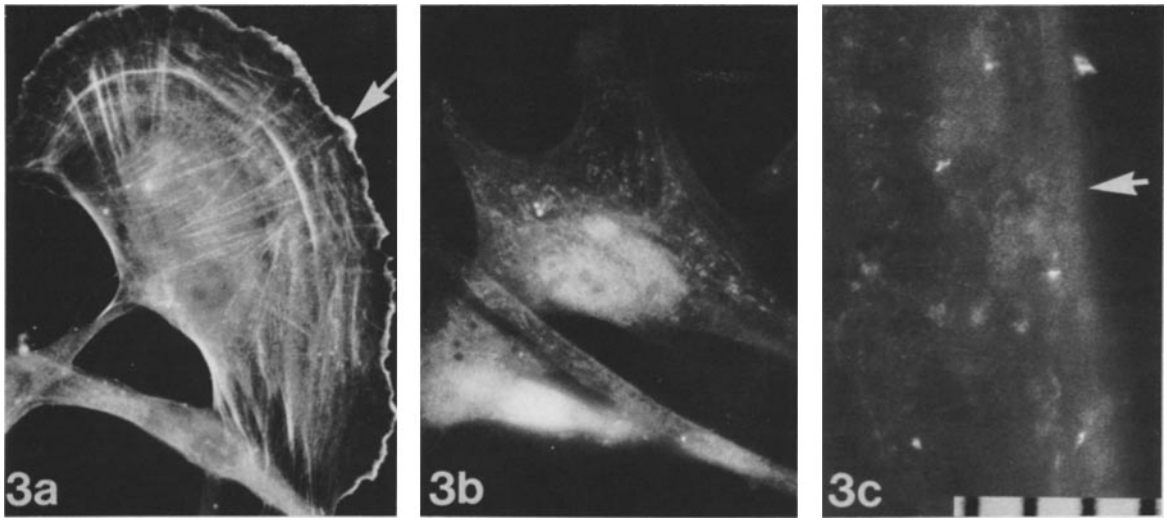

FIGURE 3 Antiactin staining in tissue culture cells and control staining. (*a*) Embryonic chick primary culture cells stained with affinity-purified antiactin and Fl-GAR. Stress fibers and membrane ruffles at the cell perimeter (arrow) are stained. (*b*) Embryonic chick primary culture cells stained with high concentrations of absorbed IgG and Fl-GAR. Note the nuclear and cytoplasmic particle staining. Stress fibers and lamellipodia do not stain. (*c*) Fish scale stained with absorbed IgG and Fl-GAR. A region near the edge of a scale (arrow) is shown. No stress fiber patterns in the scleroblasts are visible. Scale: 1 division = 10 μm.

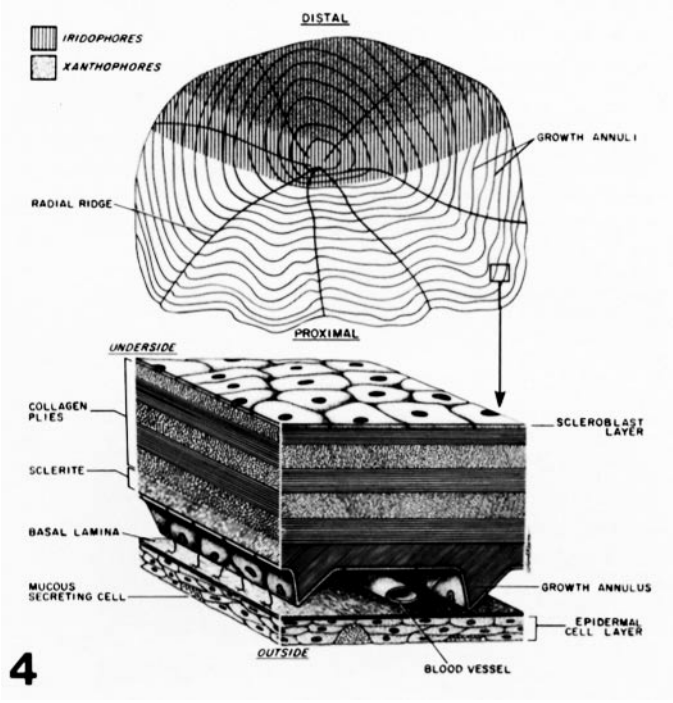

FIGURE 4 Schematic representation of the goldfish scale. The upper drawing illustrates the general architecture of the scale including the contourlike growth annuli and the radial ridges. It also shows topographic distribution of two cell types: xanthophores (yellow pigmented cells on the outer surface of the scale; the stippled area) and iridophores (cells containing reflecting platelets on the undersurface of the scale; the area indicated by parallel lines). All observations are made on the underside of the proximal half of the scale. The area demarcated by the box is enlarged and represented in the lower drawing. This drawing depicts the orientation (i.e., undersurface facing upwards) of the scale seen in the epifluorescence microscope. The undersurface of the scale is covered by a monolayer of fibroblastic cells called scleroblasts which are in intimate contact with the uppermost ply of orthogonally arranged collagen fibers (fibrillary plate). Exterior to the fibrillary plate is the partially mineralized sclerite layer, which includes the growth annuli. The sclerite is also covered by a scleroblast layer. Loose connective tissue is then encountered followed by the basal lamina and finally the epidermal cell layer that faces the external environment. The relatively flat surface of the scleroblast layer on the undersurface permits examination of stress fibers stained with specific antibodies.

described in Materials and Methods did not show such staining patterns. Cells in Fig. 3 *b* were stained with a high concentration (0.5 mg/ml) of absorbed IgG and show nonspecific staining of nuclei, cytoplasmic particles, and certain areas of the cytoplasm.

Controls for Indirect Immunofluorescence on Goldfish Scales

When goldfish scales were stained with absorbed IgG and Fl-GAR, only a low level of general fluorescence was detectable (Fig. 3 *c*). Granules of xanthophores showed autofluorescence, but this did not interfere with our studies, as we used the proximal half of the scale (see Fig. 4 for orientation). Controls for anti-alpha-actinin and antimyosin staining on the scale were also carried out as described above, except that absorbed IgG was not tested. Both preimmune sera and competition controls for these antibodies exhibited a low level of general fluorescence.

Determination of in Situ Scleroblast Shape

Scleroblasts form a thin pseudo-epithelium that surrounds the entire fibrillary plate of the fish scale, forming a continuous unicellular sheet (20, 29; Fig. 4). All images were taken on the proximal and underside of the scale where scleroblasts can be directly visualized, since in other regions the scleroblast monolayer is covered by epidermal cells, xanthophores, and iridophores (Fig. 4).

When Nomarski differential interference contrast microscopy was used, closely associated scleroblasts forming a pseudo-epithelium could be examined (Fig. 5). The contour of scleroblasts appeared smooth, indicating a lack of large cell processes. Establishing this fact is important to ensure that the fluorescent fibers revealed by immunofluorescence (Figs. 6–8)

were not cell processes. Fig. 5 also shows the collagen fibers of the scale (arrows) and the epidermal cells (*Ep*) near the edge of the scale.

Visualization of Stress Fibers in Scleroblasts in Situ

Phase-contrast images of the proximal and underside of goldfish scales (Fig. 6*a* and *c*) showed scleroblast nuclei (*N*) and the growth annuli (arrows) roughly parallel to the edge of the scale. As opposed to Nomarski differential interference contrast, phase-contrast images did not reveal boundaries of individual scleroblasts.

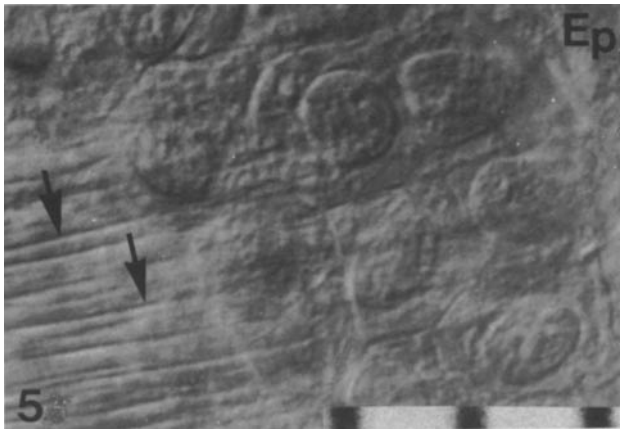

FIGURE 5 Scleroblasts showing their smooth contour. Nomarski differential interference contrast image of scleroblasts near the edge of a scale. Scleroblasts do not have cellular processes and show a smooth cell border. Note the collagen fibers (arrows) and the epidermal cells (EP) near the edge of the scale. Scale: 1 division = 10 μm.

When fish scales were stained with affinity-purified antiactin and Fl-GAR, epidermal cells showed intense and diffuse staining. Although they were situated below the focal plane during epifluorescence examination of the scleroblasts, their bright fluorescence illuminated the entire scale. This background noise reduced the contrast of the fluorescent signal in the scleroblast. In addition, the epidermal sheet was slightly exposed on the underside of the scale, thus the edges of the scales stained brightly (Fig. 6*b* and *d*). Despite these limitations, actin-containing fluorescent fibers in scleroblasts can be seen just outside and penetrating into the bright region on the edge of the scale (Fig. 6*b* and *d*, arrows). These fluorescent fibers exhibit an overall morphology similar to that of stress fibers observed in vitro. The fibers are ~0.5 μm in width and often extend 20 μm or more in length, indicating that they can span the entire length of some scleroblasts (see Fig. 5 for the size of the cells). The fibers often reside in groups and are either convergent (Fig. 6*b*, arrows) or nearly parallel (Fig. 6*d*, arrows). In contrast to microtubules (6), the antiactin staining fibers do not appear to align with collagen fibers.

Visualization of Alpha-actinin in Scleroblasts in Situ

When the fish scales were stained with anti-alpha-actinin and Fl-GAR (Fig. 7*b*), an intense fluorescence on the edge of the scale due to the epidermal cells was again visualized. In addition there were fibers exhibiting a periodicity of 1–2 μm along their length. As in the antiactin staining patterns, anti-

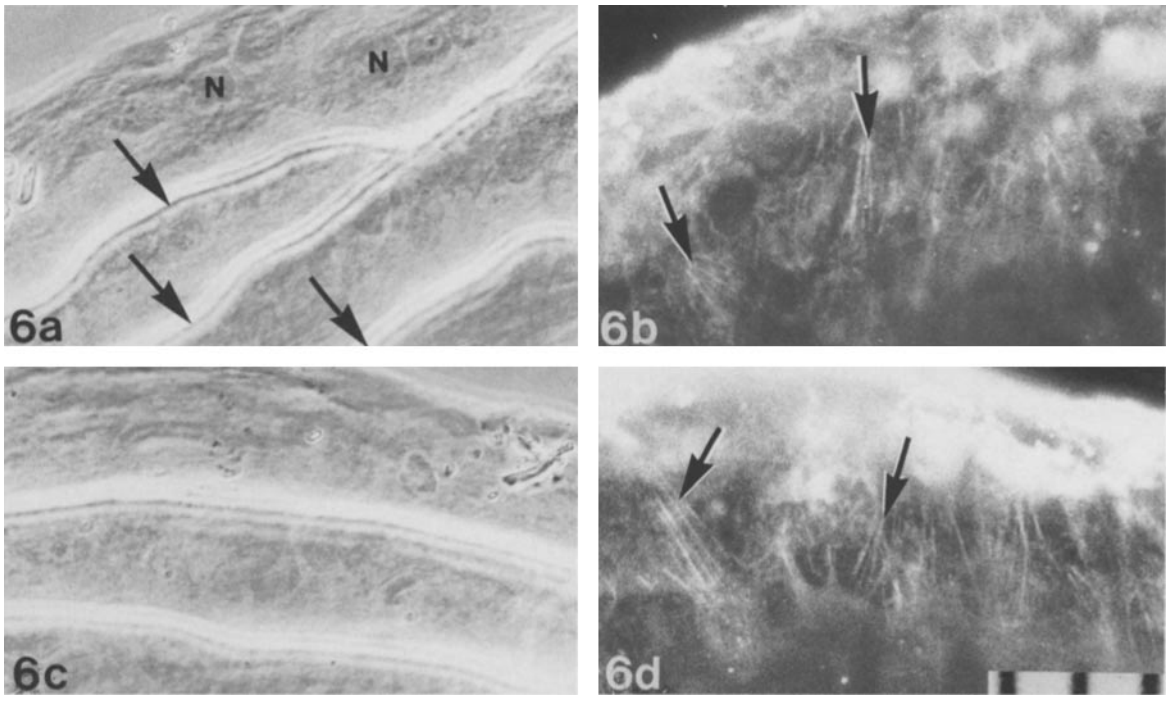

FIGURE 6 Stress fibers *in situ* in scleroblasts stained with antiactin and Fl-GAR. (*a* and *c*) Phase-contrast images of goldfish scales near the edge. Growth annuli (arrows) are roughly parallel to the edge. Nuclei (*N*) are sometimes visualized but the cell boundaries of scleroblasts cannot be distinguished. (*b*) Indirect immunofluorescent image of the scale as in *a*. Intense fluorescence near the edge of the scale is due to the epidermal layer that curves around the edge of the scale to cover part of the scleroblast layer. The scleroblasts demonstrate convergent antiactin-staining fibers (arrows) that have dimensions similar to those of stress fibers in cultured cells. These fibers are oriented roughly perpendicular to the edge of the scale. (*d*) Fluorescent image of the same region of fish scale as in *c* showing parallel stress fibers (arrows). Scale: 1 division = 10 μm.

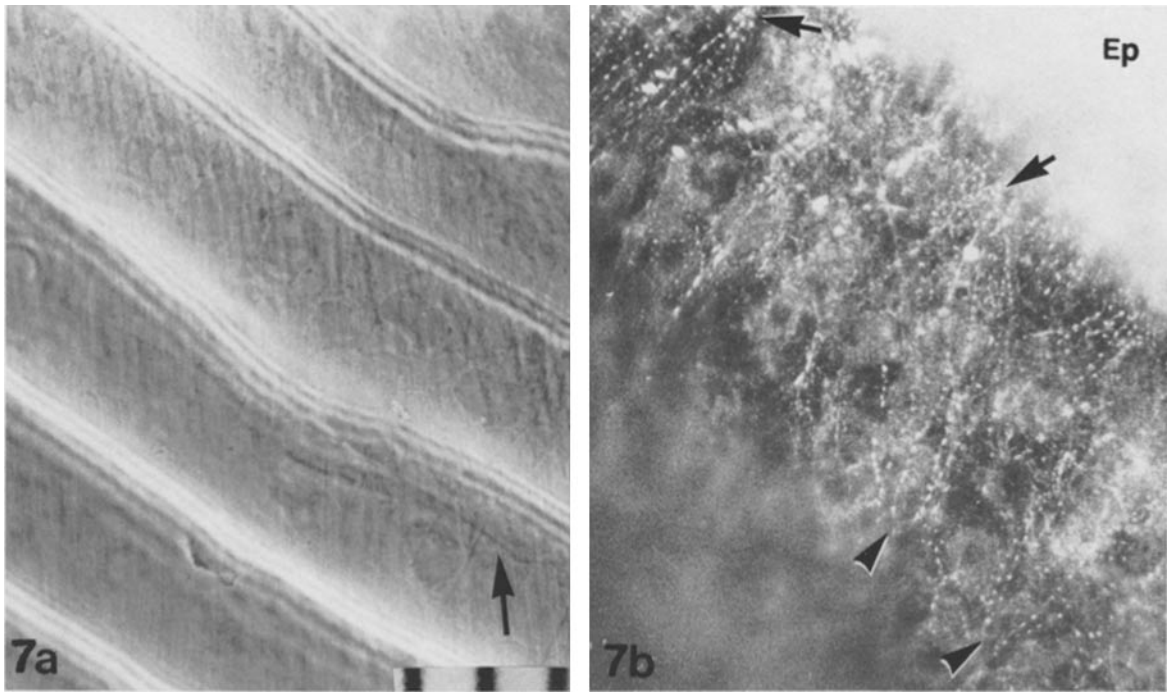

FIGURE 7 Stress fibers in scleroblasts *in situ* stained with anti-alpha-actinin and Fl-GAR. (*a*) Phase-contrast image of a goldfish scale near the edge. The arrow indicates the orientation of collagen fibers. (*b*) Region corresponding to that in *a*, showing fluorescently labeled fibers that have a distribution similar to that of actin fibers, except that they show periodic staining of 1–2 μm. The fibers are oriented perpendicular to the edge of the scale. Convergent fibers (arrows) are apparent in this region, and the point of convergence is not always towards the edge (arrowheads). The edge of the scale demonstrates intense staining in the epidermal layer (*Ep*). Scale: 1 division = 10 μm.

alpha-actinin stained parallel as well as convergent fibers. The convergence of the fibers was directed either toward (Fig. 7 *b*, arrows) or away from (Fig. 7 *b*, arrowheads) the edge of the scale. Most of the fibers were oriented perpendicular to the edge of the scale. The orientation of the fibers was independent of the direction of the collagen fibers (Fig. 7 *a*, arrow).

Visualization of Myosin in Scleroblasts in Situ

The antimyosin staining in scleroblasts was also primarily confined to fibers oriented perpendicular to the growth annuli (Fig. 8 *b*) near the edge of the scale (Fig. 8 *a*, arrowhead). Again, these fibers showed no correlation with the orthogonally arranged collagen fibers (Fig. 8 *a*, arrows). Although many fibers showed continuous fluorescence along their length, some appeared to have intermittent fluorescence (Fig. 8 *b*, arrows). Again, the periodicity was ~1–2 μm. In regions where the radiating ridges of the scale were observed (Fig. 4, and Fig. 8 *c* and *d*, *rr*), antimyosin-staining fibers were oriented perpendicular to this structure and appeared to span it (Fig. 8 *d*). A periodicity along these fibers is occasionally observed in this region as well (Fig. 8 *d*, arrow). The co-orientation of the stress fibers in Fig. 8 *d* with the direction of growth annuli and collagen fibers (Fig. 8 *c*, arrows) is coincidental, as they have no correlation in other fields.

Immunofluorescence Patterns of Scleroblast in the Central Region of the Scale

The parallel and convergent fluorescent fibers stained with antiactin and anti-alpha-actinin were rarely found in scleroblasts in the more central regions of the scale. Instead, we found meandering fibers that stained continuously with antiactin and discontinuously with anti-alpha-actinin. These fibers often formed triads, suggesting that they may represent regions of the cell margin. The orientation of collagen fibers, the growth annuli, and the radiating ridge had no relation to the pattern of these meandering fibers. Antimyosin staining in the more central regions sometimes revealed fluorescent fibers similar to those found near the edge.

DISCUSSION

Induction, Purification, and Characterization of Antiactin

That actin is a highly conserved molecule probably explains its poor antigenicity. Although autoantibodies against actin can be encountered in certain human liver diseases (13, 23), to elicit an immune response in experimental animals it is usually recommended to alter the actin molecule before injection by SDS denaturation (21, 25), by heat denaturation (31), by "aging" (36), or by glutaraldehyde fixation (17). Herman and Pollard (17) found that glutaraldehyde-fixed F-actin produced antibodies in all of five rabbits used although none of the antisera formed precipitin lines with actin in double-diffusion analysis unless the antibody was purified and concentrated by affinity chromatography. We took this approach to make antibodies against fish skeletal muscle actin.

We found that only one of the two rabbits immunized with glutaraldehyde-fixed F-actin produced antibodies. Native F-actin did not elicit antibodies even after the fourth boost. In addition, our affinity-purified antibody, even at high concentrations, still did not form precipitin lines in double-immunodiffusion analysis. Thus, our antibody is of the nonprecipitating type, due not to low titer but to an inability to form a stable

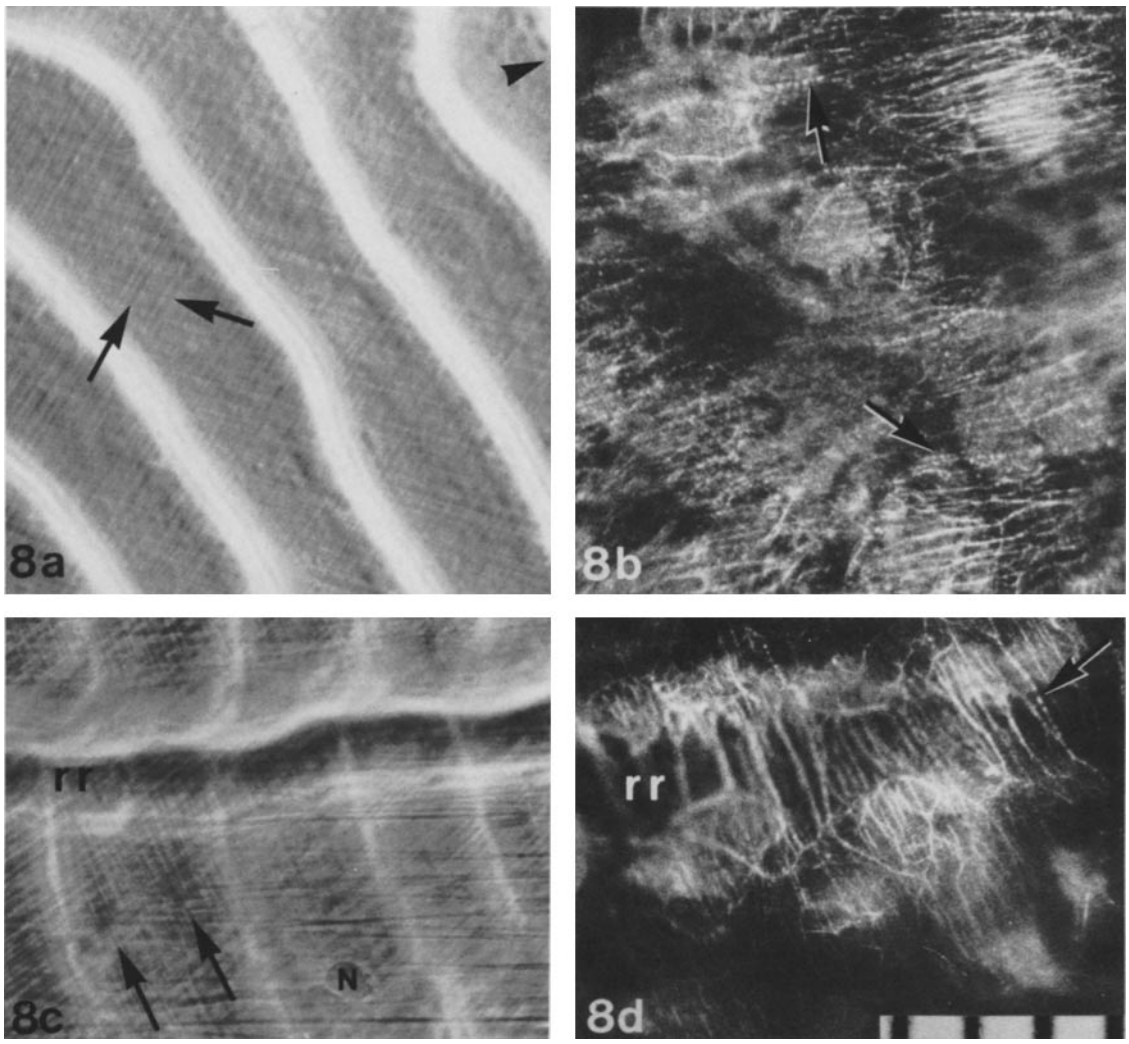

FIGURE 8 Stress fibers in scleroblasts *in situ* stained with antimyosin and Fl-GAR. (*a*) Phase-contrast image of region adjacent to the edge of the scale. Arrowhead indicates direction of edge which is parallel to the growth annuli. In this region two plys of the orthogonally arranged collagen fibers can be visualized (arrows). (*b*) Epifluorescent image of *a* showing stress fibers perpendicular to the scale edge. Occasionally, fibers demonstrate a 1- to 2-μm periodicity (arrows). (*c*) Phase-contrast image of region of the fish scale showing a radial ridge (*rr*) as well as the growth annuli, collagen fiber phase striations (arrows), and nuclei (*N*). (*d*) Epifluorescent pattern of *c* showing stress fibers that appear to span the radial ridge (*rr*). These fibers are oriented perpendicular to the radial ridge. Stress fibers with a 1- to 2-μm periodicity are occasionally observed (arrows). Scale: 1 division = 10 μm.

cross-link between actin monomers. To demonstrate the presence and the specificity of nonprecipitating antibodies, we used antigens immobilized onto nitrocellulose. The sensitivity of the electrophoretic blotting–peroxidase methods (35) is quite high. For example, when 2 μg of actin was loaded onto the microgels and roughly 10% was transferred to the nitrocellulose, it was sufficient to produce an intense reaction product.

Do Stress Fibers Exist in Cells in Situ?

Bundles of actin filaments are present in the core of the microvilli of intestinal absorptive cells (28). Tropomyosin, alpha-actinin, myosin, and filamin are localized only in the terminal web region of these cells and not along the microfilament bundles of the microvillus (2). In contrast to the composition of the microvillar core, all these proteins are associated with stress fibers in tissue culture cells. It is thus clear that microvillar actin bundles cannot be considered as a stress fiber *in situ*.

Besides the microvillar-related structures such as stereocilia and filopodia, there are relatively few examples where microfilament bundles are found in nonmuscle cells *in situ*: Sertoli cells (10), iridophores of reptiles (32), cone cells of the teleost retina (4), cuticle-forming cells of insects (30), and vascular endothelial cells (8). However, none of these microfilament bundles has been shown to have the same composition and arrangement of proteins as stress fibers in cultured cells. Several contractile proteins have been immunohistochemically localized in a variety of tissue using cryostat sections. However, none of these studies revealed filamentous distribution of the cytoskeletal proteins.

The present study has established that stress fiber–like structures can be observed by immunofluorescence in scleroblasts *in situ*. The intracellular distribution of these fibers is analogous to the convergent and parallel patterns observed in cultured cells. These fibers consist of actin, myosin, and alpha-actinin. In addition, the 1- to 2-μm periodicity exhibited by antimyosin and anti-alpha-actinin staining compares well with the periodicities observed in stress fibers in tissue culture cells. Since the distribution, dimensions, and composition of these fibers are

similar to those of stress fibers, we have chosen to also term them stress fibers.

Significance of Stress Fibers in Situ

Scleroblasts reside on the fish scale and are intimately associated with the orthogonally arranged collagen fibers of the fibrillary plate. They are believed to be responsible for the synthesis of the collagen (20, 29). We previously found a coalignment of microtubules with the collagen fibers, suggesting that microtubules may play a role in the organization of collagen fibrils of the fish scale (6). However, the present study shows that the orientation of stress fibers is independent of the directionality of the collagen fibers. Whether the stress fibers are oriented with another extracellular fibrous matrix, such as fibronectin, as it is in vitro (18), remains unknown.

Stress fibers are specifically located at the edge of the scale and elevated ridges where greater shearing forces are expected to be encountered at an interface between a rigid medium (fibrillary plate) and a less rigid medium (loose connective tissue). This finding may suggest that scleroblasts form stress fibers so that cell adhesivity is increased in these regions. This hypothesis is consistent with the fact that stress fibers in tissue culture cells are important for enhanced cell adhesion to the substrate. However, it is interesting to note that the majority of scleroblasts do not exhibit stress fibers and yet they are extremely flat and well-attached to the fibrillary plate. Recent studies have indicated that, while most vascular endothelial cells *in situ* do not have stress fibers, cells located in the area where increased shear force is expected can develop stress fibers (38, 39). These findings indicate that *in situ* cells use a different mechanism for adhesion and that stress fibers develop only when increased adhesion is necessary.

We would like to thank Drs. K. R. Porter, M. Mooseker, R. Linck, S. Ito, and G. White for practical and inspirational support. We would especially like to thank David Paul and Janet Lyons for allowing us to use the nitrocellulose disk technique before publication of their work and also for their help with the electrophoretic blotting and peroxidase techniques.

This paper was funded by National Institutes of Health (NIH) training grant GM 07753 to H. R. Byers and NIH grants GM 25637 to K. Fujiwara and GM 24121 to K. R. Porter.

This study was presented at the 21st Annual Meeting of the American Society for Cell Biology, Anaheim, CA (November 1981) (5).

Received for publication 21 September 1981, and in revised form 18 January 1982.

REFERENCES

1. Bragina, E. E., Ju. M. Vasiliev, I. M. Gelfand. 1976. Formation of bundles of microfilaments during spreading of fibroblasts on the substrate. *Exp. Cell Res.* 97:241–248.
2. Bretscher, A., and K. Weber. 1978. Localization of actin and microfilament-associated proteins in microvilli and terminal web of intestinal brush-border by immunofluorescence microscopy. *J. Cell Biol.* 79:839–845.
3. Buckley, I. K., and K. R. Porter. 1967. Cytoplasmic fibrils in living cultured cells. A light and electron microscope-study. *Protoplasma.* 64:349–380.
4. Burnside, B. 1978. Thin (actin) and thick (myosinlike) filaments in cone contraction in the teleost retina. *J. Cell Biol.* 78:227–246.
5. Byers, H. R., and K. Fujiwara. 1981. Immunofluorescent identification of stress fibers and microtubules in fish scales *in situ*. *J. Cell Biol.* 91 (2, Pt. 2):307 *a* (Abstr.).
6. Byers, H. R., K. Fujiwara, and K. R. Porter. 1980. Visualization of microtubules of cells *in situ* by indirect immunofluorescence. *Proc. Natl. Acad. Sci. U. S. A.* 77:6657–6661.
7. Cuatrecasas, P. 1970. Protein purification by affinity chromatography. Derivatizations of agarose and polyacrylamide beads. *J. Biol. Chem.* 145:3059–3065.
8. De Bruyn, P. P. H., and Y. Cho. 1974. Contractile structures in endothelial cells of splenic sinusoids. *J. Ultrastruct Res.* 49:24–33.
9. Feramisco, J. R. 1979. Microinjection of fluorescently labeled alpha-actin into living fibroblasts. *Proc. Natl. Acad. Sci. U. S. A.* 76:3967–3971.
10. Franke, W. W., C. Grund, A. Fink, and K. Weber. 1978. Location of actin in microfilament bundles associated with junctional specializations between sertoli cells and spermatids. *Biol. Cell.* 31:7–14.
11. Fujiwara, K., and T. D. Pollard. 1976. Fluorescent antibody localization of myosin in the cytoplasm, cleavage furrow, and mitotic spindle of human cells. *J. Cell Biol.* 71:848–875.
12. Fujiwara, K., M. E. Porter, and T. D. Pollard. 1978. Alpha-actinin localization in the cleavage furrow during cytokinesis. *J. Cell Biol.* 79:268–275.
13. Gabbiani, G., G. B. Ryan, J. P. Lamelin, P. Vassali, G. Majno, C. A. Bouvier, A. Gruchand, and E. F. Luscher. 1973. Human smooth muscle antibody. Its identification as anti-actin antibody and a study of its binding to non-muscle cells. *Am. J. Pathol.* 72:473–488.
14. Goldman, R. D. 1971. The role of three cytoplasmic fibers in BHK-21 cell motility. I. Microtubules and the effects of colchicine. *J. Cell Biol.* 51:752–762.
15. Goldman, R. D., C. Chang, and J. Williams. 1974. Properties and behavior of hamster embryo cells transformed by human adenovirus type 5. *Cold Spring Harbor Symp. Quant. Biol.* 39:601–614.
16. Gotlieb, A. 1979. Mechanochemical proteins, cell motility and cell-cell contacts: the localization of mechanochemical proteins inside cells at the edge of an *in vitro* "wound." *J. Cell Physiol.* 100:563–578.
17. Herman, I. M., and T. D. Pollard. 1979. Comparison of purified anti-actin and fluorescent-heavy meromyosin staining patterns in dividing cells. *J. Cell Biol.* 80:509–520.
18. Hynes, R. D., and A. T. Destree. 1978. Relationships between fibronectin (LETS protein) and actin. *Cell.* 15:875–886
19. Ishikawa, H., R. Bischoff, and H. Holtzer. 1969. Formation of arrowhead complexes with heavy meromyosin in a variety of cell types. *J. Cell Biol.* 43:312–328.
20. Junqueira, L. C. U., A. M. S. Toledo, and K. R. Porter. 1970. Observations on the structure of the skin of the teleost, *Fundulus heteroclitus* (2). *Arch Histol. Jpn.* 32:1–15.
21. Kleve, M. G., J. W. Fuseler, and W. H. Clark, Jr. 1979. Antibodies against invertebrate actin: their phylogenetic cross-reactivity. *J. Exp. Zool.* 209:21–32.
22. Kreis, T. E., K. H. Winterhalter, and Birchmeier, W. 1979. In vivo distribution and turnover of fluorescently labeled actin microinjected into human fibroblasts. *Proc. Natl. Acad. Sci. U. S. A.* 76:3814–3818.
23. Kurki, P. 1978. Determination of anti-actin antibodies by a solid phase immunoenzymatic assay and by indirect immunofluorescence technique. *Clin. Immunol. Immunopathol.* 11:328–338.
24. Laemmli, U. K. 1970. Cleavage of structural proteins during the assembly of the head of bacteriophage T4. *Nature (Lond.).* 227:680–685.
25. Lazarides, E. 1975. Tropomyosin antibody: the specific localization of tropomyosin in non-muscle cells. *J. Cell Biol.* 65:549–561.
26. Lazarides, E., and K. Burridge. 1975. Alpha-actinin: immunofluorescent localization of a muscle structural protein in non-muscle cells. *Cell.* 6:289–298.
27. Lazarides, E., and K. Weber. 1974. Actin antibody: the specific visualization of actin filaments in non-muscle cells. *Proc. Natl. Acad. Sci. U. S. A.* 71:2268–2272.
28. Mooseker, M. S., and L. G. Tilney. 1975. Organization of an actin filament membrane complex. Filament polarity and membrane attachment in microvilli of intestinal epithelial cells. *J. Cell Biol.* 67:725–743.
29. Onozato, H., and N. Watabe. 1979. Studies on fish scale formation and resorption. *Cell Tissue Res.* 201:409–422.
30. Overton, J. 1966. Microtubules and microfilaments in morphogenesis of the scale cells of *Ephestia kühniella*. *J. Cell Biol.* 29:293–305.
31. Owen, M. J., J. Auger, B. H. Barber, A. J. Edwards, F. S. Walsh, and M. J. Crumpton. 1978. Actin may be present on the lymphocyte surface. *Proc. Natl. Acad. Sci. U. S. A.* 75:4484–4488.
32. Rohrlich, S. T., and K. R. Porter. 1972. Fine structural observations relating to the production of color by the iridophores of a lizard, *Anolis carolinensis*. *J. Cell Biol.* 53:38–52.
33. Spooner, B. S., K. M. Yamada, and N. K. Wessells. 1971. Microfilaments and cell locomotion. *J. Cell Biol.* 49:595–613.
34. Spudich, J. A., and S. Watt. 1971. The regulation of rabbit skeletal muscle contraction. I. Biochemical studies of the interaction of the tropomyosin-troponin complex with actin and the proteolytic fragments of myosin. *J. Biol. Chem.* 146:4866–4871.
35. Towbin, H., T. Staehelin, and J. Gordon. 1979. Electrophoretic transfer of proteins from polyacrylamide gels to nitrocellulose sheets: procedures and some applications. *Proc. Natl. Acad. Sci. U. S. A.* 76:4350–4354.
36. Trencher, P., and E. J. Holobrow. 1976. The specificity of anti-actin serum. *Immunology.* 31:509–517.
37. Wehland, J., M. Osborn, and K. Weber. 1979. Cell to substratum contacts in living cells, a direct correlation between interference reflexion and indirect immunofluorescence microscopy using antibodies against actin and alpha-actin. *J. Cell Sci.* 37:257–273.
38. White, G. E., K. Fujiwara, E. J. Shefton, C. F. Dewey, and M. A. Gimbrone, Jr. 1982. Fluid shear influences cell shape and cytoskeletal organization in cultured vascular endothelium. *Fed. Proc.* 41:321.
39. Wong, A. J., T. D. Pollard, and I. M. Herman. 1981. Endothelial cells contain stress fibers *in vivo*. *J. Cell Biol.* 91 (2, Pt. 2):299 *a* (Abstr.).